analytical chemistry

Article

pubs.acs.org/ac

Characterization of Copolymers and Blends by Quintuple-Detector Size-Exclusion Chromatography

Steven M. Rowland[†] and André M. Striegel*[,‡]

[†]Department of Chemistry & Biochemistry, Florida State University, Tallahassee, Florida 32306-4390, United States

[‡]Analytical Chemistry Division, National Institute of Standards and Technology, 100 Bureau Drive, Mail Stop 8392, Gaithersburg, Maryland 20899, United States

Supporting Information

ABSTRACT: The properties imparted, oftentimes synergistically, by the different components of copolymers and blends account for the widespread use of these in a variety of industrial products. Most often, however, processing and end-use of these materials (especially copolymers) is optimized empirically, due to a lack of understanding of the physicochemical phase-space occupied by the macromolecules. Here, this shortcoming is addressed via a quintuple-detector size-exclusion chromatography (SEC) method consisting of multiangle static light scattering (MALS), quasi-elastic light scattering (QELS), differential viscometry (VISC), ultraviolet absorption spectroscopy (UV), and differential refractometry (DRI) coupled online to the separation method. Applying the SEC/MALS/QELS/VISC/UV/DRI method to the study of a poly(acrylamide-*co*-*N*,*N*-dimethylacrylamide) copolymer in which both monomer functionalities absorb in the same region of the UV spectrum, we demonstrate how to determine the chemical heterogeneity, molar mass averages and distribution, and solution conformation of the copolymer all in a single analysis. Additionally, through the various mutually independent conformational and architectural metrics provided by combining the five detectors, including the fractal dimension (derived from two different detector combinations), two different dimensionless size parameters, the chemical heterogeneity, and the persistence length, it is shown that the monomeric arrangement is more alternating than random at lower molar masses, thus causing the copolymer to adopt a more extended conformation in solution in this molar mass (M) regime. At high M, however, the copolymer is shown to be and to behave more like a random coil homopolymer, after passing through a 250 kg mol^{-1}-broad region of intermediate chain flexibility. Thus, the combination of five detectors provides a unique means by which to determine absolute properties of the copolymer, solution-specific physical behavior, and the underlying chemical basis of the latter. The quintuple-detector method was also extended to the study of blends of polyacrylamide and poly(*N*,*N*-dimethylacrylamide) homopolymers to quantitate their molar mass, solution conformation, and chemical heterogeneity and to shed light on the breadth of the distributions of the component species. The method presented should be applicable to the study of copolymers and blends in which either one or both component moieties or polymers absorb in the UV region and can be implemented using not only SEC but other size-based separation methods as well.

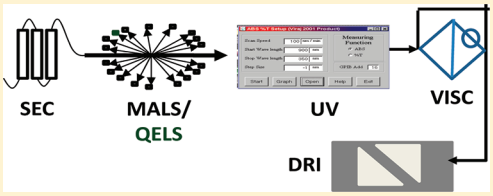

Since the mid-1960s, when Moore first published on gel-permeation chromatography (GPC, now better known as size-exclusion chromatography, SEC),[1−5] polymer scientists have understood that with suitable calibration techniques size-based separations could provide precise and accurate molar mass averages and distributions (MMD) of polymers. However, in order to construct an accurate calibration curve, information is needed about the size, shape, and architecture of both the calibrants and analytes in solution. The advent of online static light scattering (SLS) detection,[6] in particular of multiangle static light scattering (MALS) photometry,[7] provided a method which, when combined with a size-based separation, could determine molar mass and size without the use of calibration curves or the need for *a priori* knowledge of polymer size, shape, or topology.[2−5] Although SLS detection provides valuable molar mass and size information, multidetector separations are necessary to accurately characterize polymers with complex heterogeneities in molar mass, chemical composition, and conformation.

"Chemical heterogeneity" is the term used to denote the change, or lack thereof, in the ratio of the functionalities of a copolymer or of the components in a blend, as a function of analyte (copolymer or blend) molar mass. Chemical heterogeneity has been shown to influence physical properties such as the strength between polymer−polymer interfaces,[8] conductivity,[9] polymer release properties in pharmaceuticals,[10] adsorption at the interface of immiscible liquids,[11] and SEC separation processes and the information derived therefrom.[12,13] Previous measurements of chemical heterogeneity relied on a variety of on- and off-line techniques such as off-line infrared spectroscopy,[14] interactive and size-based separations coupled to flow-

Received: February 8, 2012
Accepted: May 1, 2012
Published: May 16, 2012

   dx.doi.org/10.1021/ac3003775 | *Anal. Chem.* 2012, 84, 4812−4820

through nuclear magnetic resonance (NMR) spectroscopy,[15,16] SEC with off-line NMR and mass spectrometry,[17] gradient liquid chromatography,[18] and multidetector SEC for studying copolymers in which only one component absorbs in the UV region.[12]

In this work, we propose a quintuple-detector SEC separation in which a combination of MALS, quasi-elastic light scattering (QELS), UV spectroscopy, differential viscometry (VISC), and differential refractive index (DRI) detection was used to simultaneously determine the chemical heterogeneity, molar mass averages, and MMD of copolymers and blends, as well as the molar mass dependence of the macromolecular radii, intrinsic viscosity, fractal dimension, and solution conformation of the samples. The method applies to copolymers or binary blends in which both functionalities or components absorb in the same region of the UV spectrum, a distinct advantage over previous spectroscopic-absorption-based approaches to the determination of chemical heterogeneity in copolymers, where only one absorptive component could be present if quantitation was desired.[12,19]

By allowing an analyte to be examined from a multiplicity of mutually independent vantage points (i.e., based on both optical and transport or hydrodynamic properties), the method presented here provides a clearer and more complete picture of copolymers and blends than that usually presented in the literature using a single technique (or, oftentimes, even using several techniques), while employing separation and detection techniques common to most macromolecular separations laboratories. The method presented should therefore prove of interest to those designing, synthesizing, and analyzing copolymers and blends for a variety of purposes.

EXPERIMENTAL SECTION

Materials. Poly(acrylamide) (PAM), poly(*N*,*N*-dimethylacrylamide) (PDMAM), and a random poly(acrylamide-*co*-*N*,*N*-dimethylacrylamide) copolymer were obtained from Polymer Source (Dorval, Quebec, Canada). Mobile phase and solvent were deionized H_2O with 0.5 mol L^{-1} acetic acid and 0.5 mol L^{-1} NaCl, vacuum filtered through a 0.2 μm nylon filter.

Quintuple-Detector Size-Exclusion Chromatography (SEC/MALS/QELS/VISC/UV/DRI). Size-exclusion chromatography was performed with a Waters 2695 Separations Module (Waters, Milford, MA) with an online degasser, an online preinjection 0.2 μm nylon filter, and four Agilent/Polymer Laboratories (Santa Clara, CA) columns connected in series, PL Aquagel-OH 60, 50, 40, and 30 (it should be noted that the pore volumes of these columns differ from each other by only a few percent, as reported by the manufacturer, thus obviating pore mismatch issues). The total separation range of the columns, as reported by the manufacturer, is 1×10^2 to 1×10^7 g mol^{-1} based on estimates using polyethylene oxide/polyethylene glycol (PEO/PEG) standards in aqueous solution at room temperature. Separations in our lab were performed at a flow rate of 1 mL min^{-1} using the aqueous mobile phase described above. Sample injection volume was 100 μL, concentration was 3 mg mL^{-1} (0.7 and 1.0 mg mL^{-1} solutions produced similar, albeit noisier, results), and column and detector temperatures were maintained at 30 °C.

The multidetector SEC system incorporated five detectors connected in series: A DAWN EOS multiangle static light scattering photometer (Wyatt Technology Corp., Santa Barbara, CA), a quasi-elastic light scattering photometer (Wyatt), a model 166 UV detector (Beckman-Coulter, Fullerton, CA), a ViscoStar differential viscometer (Wyatt), and an Optilab rEX differential refractometer (Wyatt). The MALS and QELS units were contained in the same housing. The UV detector was set to a wavelength of 240 nm, where *N*,*N*-dimethylacrylamide absorbs preferentially over acrylamide (see Off-Line Determination of Absorptivities, below). A narrow dispersity dextran sample with a molar mass of 15 000−20 000 g mol^{-1} was used for normalization of the MALS photodiodes and for calculating interdetector delays and interdetector band broadening corrections.[20] Data acquisition was performed with Wyatt's ASTRA software (V.5.3.4.18), with static light scattering calculations performed by applying the Zimm model. Calculations and plotting were performed with Microsoft Office Excel 2007 (Microsoft Corp., Redmont, WA) and OriginPro 7.5 (V.7.0, Origin Lab Corp., Northampton, MA).

Off-Line Determination of Specific Refractive Index Increment $\partial n/\partial c$. The polymer samples were dissolved in mobile phase and left overnight on a wrist-action shaker to ensure complete dissolution. For off-line $\partial n/\partial c$ determination, seven dilutions of each sample, ranging from 0.2 to 1.5 mg mL^{-1}, were injected directly into the Optilab rEX differential refractometer (Wyatt) using a Razel model R99-EJ syringe pump. The flow rate was set to 0.5 mL min^{-1}. Sample solutions were filtered gently through a 0.45 μm nylon syringe filter before injection. The vacuum wavelength of the DRI was 685 nm (within 5 nm of that of the MALS photometer in the SEC experiments). Data acquisition and processing were done with Wyatt's ASTRA software (V.5.3.4.18). The $\partial n/\partial c$ values for PAM and PDMAM were 0.162 ± 0.009 mL g^{-1} and 0.150 ± 0.003 mL g^{-1}, respectively. The $\partial n/\partial c$ for the bulk copolymer was calculated from the bulk percent composition, as provided by the manufacturer, to be 0.155 ± 0.009 mL g^{-1} (as noted in the Results and Discussion section, the presence of chemical heterogeneity results in a $\partial n/\partial c$ heterogeneity in the copolymer).

The $\partial n/\partial c$ values of the homopolymers determined by off-line DRI agreed closely with the same values determined by using the refractometer as an online SEC detector and assuming 100% mass recovery from the column. For samples which may exhibit polyelectrolytic behavior, it has been demonstrated that $\partial n/\partial c$ obtained by online SEC/DRI are equivalent to the same values obtained by off-line DRI after dialyzing the samples and using the dialysate as a reference solvent.[21,22] The similarity in the $\partial n/\partial c$ values obtained by on- and off-line DRI indicates that, at the given experimental conditions, the polyelectrolytic behavior of the homopolymers is, at best, minimal.

Off-Line Determination of Absorptivities. Absorptivities were determined using a Varian Cary 300 Bio UV−visible spectrophotometer (Agilent Technologies, Santa Clara, CA). Four dissolutions of poly(acrylamide) and poly(*N*,*N*-dimethylacrylamide), each ranging from 0.5 to 1.5 mg mL^{-1}, were prepared in the same manner as solutions for $\partial n/\partial c$ determination and measured at 240 nm, in triplicate. Absorptivities for PAM and PDMAM were 84 ± 1 and 1913 ± 1 mL mg^{-1} cm^{-1}, respectively.

RESULTS AND DISCUSSION

The quintuple-detector SEC system described in the Experimental Section was used to characterize a random poly(AM-*co*-DMAM) copolymer as well as physical blends of the PAM and PDMAM homopolymers. SEC was employed to

dx.doi.org/10.1021/ac3003775 | Anal. Chem. 2012, 84, 4812−4820

ensure a size-based separation, while the five-detector combination was necessary not only for determination of molar mass, size, and chemical heterogeneity but also for the determination of polymer conformation via four different parameters: the fractal dimension (d_f) from the R_G conformation plot and from the Mark–Houwink plot, each; the ρ parameter, defined as the dimensionless ratio of the radius of gyration R_G to the hydrodynamic radius R_H; and a second dimensionless size parameter, the ratio of the viscometric radius R_η to R_G. These parameters, and the information obtained therefrom, are explored more fully below, wherein we discuss the characterization of the copolymer, followed by that of the polymer blends.

Determination of Chemical Heterogeneity. Chemical heterogeneity is a common occurrence with polymerization processes such as free radical copolymerization, especially when the incorporated monomers have differing reactivities, which leads to a biased rate of incorporation into the growing chain.[12] This bias, in turn, results in chemical heterogeneity, which affects the accuracy with which molar mass, concentration, size, and conformation are determined, through the effect of chemical heterogeneity on the $\partial n/\partial c$ heterogeneity of a copolymer or blend.

The specific refractive index increment $\partial n/\partial c$ of a copolymer can generally be represented as the sum of the weight fractions w of the component comonomers, with each weight fraction multiplied by the $\partial n/\partial c$ of the respective homopolymer.[23] This relation is represented for poly(AM-*co*-DMAM) in eq 1:

$$\left(\frac{\partial n}{\partial c}\right)_{P(\text{AM-}co\text{-DMAM})} = \left(\frac{\partial n}{\partial c}\right)_{\text{PAM}} w_{\text{AM}} + \left(\frac{\partial n}{\partial c}\right)_{\text{PDMAM}} w_{\text{DMAM}} \quad (1)$$

Conventionally, a $\partial n/\partial c$ value is calculated by first measuring the DRI response for a series of dilute polymer solutions of differing concentration, as detailed in the Experimental Section for the copolymer and for the PAM and PDMAM homopolymers.[24] The slope of a plot of differential refractive index versus polymer concentration corresponds to the $\partial n/\partial c$ of the polymer at the given experimental conditions. For homopolymers with no oligomeric components, the $\partial n/\partial c$ obtained by this method is accurate for all molar masses (all slices eluting from the SEC column) because the monomer functionality is 100% at all molar masses. For chemically heterogeneous copolymers, however, the comonomer ratio (percent composition) is not the same at all molar masses, (an example of this can be seen in Figure 1). As a result of this heterogeneity in percent composition, the $\partial n/\partial c$ values will vary with molar mass and any parameter that depends on $\partial n/\partial c$ will be calculated inaccurately. Because of the small difference in $\partial n/\partial c$ between PAM and PDMAM, corrections applied to the work presented here resulted in changes in the molar mass averages and in the slopes of the conformation and Mark–Houwink plots of, at most, 2.5%. However, previous work has shown that not accounting for chemical heterogeneity can result in errors in calculated molar mass of up to ≈10% and in changes in the slopes of conformation and Mark–Houwink plots of approximately 8% and 15%, respectively.[12] The magnitude of these errors will increase either with increasing M, with increasing difference between the $\partial n/\partial c$ values of the copolymer or blend constituents, or as both these cases occur simultaneously. All statistical averages of molar mass, size, and intrinsic viscosity for the poly(AM-*co*-DMAM) copolymer

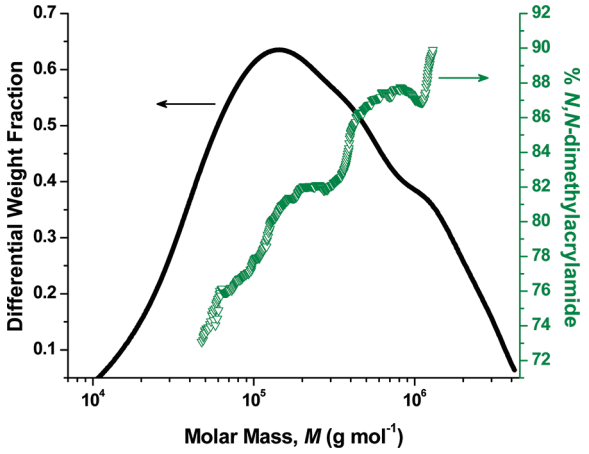

Figure 1. Chemical heterogeneity (green inverted triangles), plotted as percent mass fraction *N*,*N*-dimethylacrylamide (% DMAM) and molar mass distribution (solid black line) for a poly(acrylamide-*co*-*N*,*N*-dimethylacrylamide) copolymer, as determined using the MALS, UV, and DRI detectors of the quintuple-detector setup.

which are given here have been corrected for chemical heterogeneity by incorporating the chemical heterogeneity determined using the quintuple-detector approach presented here into the correction formulas previously derived by Haidar Ahmad and Striegel.[12]

Chemical heterogeneity was determined here according to eq 2, which was derived (as shown in the Supporting Information) to determine percent composition of monomers for a two-component copolymer or binary polymer blend in which both monomers absorb in the same UV region. For the present cases, determination is performed as percent mass fraction *N*,*N*-dimethylacrylamide (% DMAM), at each SEC elution slice i.

$$\%\text{DMAM}_i = \left\{\left(S_{\text{R,copolymer},i}\left(\frac{\partial n}{\partial c}\right)_{\text{PAM}} - Z_{\text{PDMAM}} a_{\text{PAM}}\right) \Big/ \left(Z_{\text{PDMAM}}(a_{\text{PDMAM}} - a_{\text{PAM}}) + S_{\text{R,copolymer},i}\left[\left(\frac{\partial n}{\partial c}\right)_{\text{PAM}} - \left(\frac{\partial n}{\partial c}\right)_{\text{PDMAM}}\right]\right)\right\} \times 100\% \quad (2)$$

where $S_{\text{R,copolymer},i} = S_{\text{UV},i}/S_{\text{DRI},i}$, a = absoptivity of homopolymer samples, and

$$Z_{\text{PDMAM}} = \frac{S_{\text{UV,PDMAM}}}{S_{\text{DRI,PDMAM}}} \times \frac{\left(\frac{\partial n}{\partial c}\right)_{\text{PDMAM}}}{a_{\text{PDMAM}}} = S_{\text{R,PDMAM}} \times \frac{\left(\frac{\partial n}{\partial c}\right)_{\text{PDMAM}}}{a_{\text{PDMAM}}}$$

In eq 2, Z_{PDMAM} is the product of the ratio of UV to DRI signals (S_{UV} and S_{DRI}, respectively) and the ratio of specific refractive index increment to absorptivity ($\partial n/\partial c$ and a, respectively), for a PDMAM homopolymer sample; a_{PAM} and a_{PDMAM} are the absorptivities of the individual homopolymers; and $S_{\text{R,copolymer},i}$ is the ratio of UV to DRI signals for the copolymer sample at each elution slice i. It should be noted that the use of the ratio Z_{PDMAM} in eq 2 removes the instrument constant for the online

dx.doi.org/10.1021/ac3003775 | *Anal. Chem.* 2012, 84, 4812–4820

Table 1. Chemical-Heterogeneity-Corrected Number- (*n*-), Weight- (*w*-), and *z*-Averages for Molar Mass, Radius of Gyration, Hydrodynamic Radius, and Viscometric Radius of the Poly(AM-*co*-DMAM) Sample, Determined Using SEC/MALS/QELS/UV/VISC/DRI

	number-average	weight-average	*z*-average
molar mass (g/mol)	$1.06 \times 10^5 \pm 0.08 \times 10^5$	$5.33 \times 10^5 \pm 0.85 \times 10^5$	$1.52 \times 10^6 \pm 0.17 \times 10^5$
R_G (nm)[a]	11 ± 2	29 ± 1	55 ± 2
R_η (nm)[a,b]	9 ± 2	19 ± 3	38 ± 3
R_H (nm)[a,c]	8 ± 1	18 ± 1	37 ± 1

[a]At solvent and temperature conditions as specified in the Experimental Section. Standard deviations based on replicate injections from duplicate dissolutions, as specified in the Experimental Section. [b]From $R_\eta = (3[\eta]M/10\pi N_A)^{1/3}$, where N_A is Avogadro's number. [c]From $R_H = k_B T/(6\pi\eta_0 D_T)$, where k_B is Boltzmann's constant, T is the absolute temperature of the experiment, η_0 is the viscosity of the solvent at the experimental conditions, and D_T is the translational diffusion coefficient of the analyte.

UV detector from the equation (see the Supporting Information), meaning that absorptivity values for the homopolymers can be measured on a separate (i.e., different from the online UV detector used in the SEC experiement) benchtop UV−vis spectrophotometer, provided the absorptivities of both homopolymers are measured with the same instrument. When the latter requirement is fulfilled, the instrument constant cancels out of the equation, thus obviating the need to determine instrument constants for either the online or benchtop detectors. The determination of % DMAM at each molar mass slice (i.e., at each SEC elution slice *i*) via eq 2 allows for the % DMAM to be plotted across MMD, i.e., for a plot of chemical heterogeneity to be constructed. Only the % DMAM is plotted as a function of molar mass in Figure 1, which shows that chemical heterogeneity is, indeed, present in the poly(AM-*co*-DMAM) copolymer, as % DMAM increases from ≈72% to 90% as a function of increasing *M*. Because there are only two comonomers in the sample, the weight percent acrylamide at each elution slice (% AM_i) is easily determined from the relation % AM_i = 100% − % $DMAM_i$.

Molar Mass and Radii Determination. Molar mass can be determined by SEC with the use of static light scattering (SLS) and differential refractive index (DRI) detectors. The dependence of molar mass on the signals from these two detectors and on the specific refractive index increment, at each SEC elution slice *i*, is shown in eq 3:

$$M_i \propto \frac{S_{SLS,i}}{S_{DRI,i}} \times \frac{1}{\left(\frac{\partial n}{\partial c}\right)_i} \tag{3}$$

where S_{SLS} is the signal from the MALS photometer and S_{DRI} is the signal from the DRI. As detailed earlier, a multiangle static light scattering (MALS) photometer was the type of SLS detector employed in the present set of experiments.

The ability of SLS/DRI to calculate molar mass in conjunction with the use of a size-based separation such as SEC allows determination of the MMD. The molar mass distribution of the poly(AM-*co*-DMAM) sample examined is shown in Figure 1. Molar mass averages (statistical moments of the MMD) can also be calculated when using SLS and DRI with a size-based separation. The three most commonly used molar mass averages are the number-, weight-, and *z*-average molar masses (M_n, M_w, and M_z, respectively), calculated according to[2]

$$M_\beta = \frac{\sum c_i M_i^{\,x}}{\sum c_i M_i^{\,x-1}}$$
$$(\text{when } x = 0,\ \beta = n;\ \text{when } x = 1,$$
$$\beta = w;\ \text{when } x = 2,\ \beta = z) \tag{4}$$

where c_i is the polymer concentration at elution slice *i*, determined using the DRI detector; and M_i is the molar mass determined from MALS for the same slice subsequent to correction for interdetector delay. The molar mass averages of the poly(AM-*co*-DMAM) sample studied here are listed in Table 1. The data in the table have been corrected for chemical heterogeneity based on corrections for *M* at each elution slice *i* though, as mentioned earlier, for this copolymer the corrections were only ≈2% to 3% due to the similarity in the $\partial n/\partial c$ values of the constituent homopolymers (see the Experimental Section).

The *n*-, *w*-, and *z*-averages of various radii of the poly(AM-*co*-DMAM) sample are also listed in Table 1.Three radii were calculated for the copolymer: The radius of gyration (R_G), the hydrodynamic radius (R_H), and the viscometric radius (R_η). R_G is a statistical radius that is calculated from the MALS signals, while R_H and R_η are both hard-sphere-equivalent radii calculated from QELS and from VISC/MALS/DRI signals, respectively.[2,25] These radii not only provide information about the size of the copolymer but, when combined with other parameters, can also provide structural and architectural information. Four architectural determinations will be discussed in the following subsection.

Determination of Polymer Architecture. The quintuple-detector separation approach employed here provides information about polymer architecture via the R_G and R_H conformation plots, the Mark−Houwink plot, and plots of the *M*-dependence of the dimensionless parameters ρ and $R_{\eta,w}/R_{G,z}$. To ensure accurate construction of these plots and, therefore, accurate determination of the architecture of the copolymer and blends, it is necessary to utilize the UV and DRI detectors to determine and correct for chemical heterogeneity. The R_G conformation plot of R_G versus *M*, with each axis plotted on a logarithmic scale, employs information from the MALS and DRI detectors and is based on the relationship $R_G = kM^\alpha$. Expressed in logarithmic fashion, this relation provides the equation of a straight line:

$$\log R_G = \alpha \log M + \log k \tag{5}$$

with a slope of α and *y*-intercept of log *k*.

To determine the solution conformation of the copolymer via the R_G conformation plot, we utilize the relationship between the fractal dimension (d_f) and the slope (α) of this

dx.doi.org/10.1021/ac3003775 | Anal. Chem. 2012, 84, 4812−4820

plot, namely, $d_f \equiv 1/\alpha$.[2,4] Fractal dimensions are particularly useful, as they provide a deeper insight into polymer topology than can be obtained from, e.g., the Euclidean dimension. For example, a rigid rod and a random coil both have a Euclidean dimension of 1, rendering them indistinguishable from each other via this metric. However, a comparison of fractal dimensions shows that, while the rigid rod has a d_f of 1 (although, strictly speaking, a rigid rod is not a fractal object), the random coil has a d_f between 1.67 and 2, depending on solvent and temperature conditions.

Figure 2 shows the R_G conformation plot for poly(AM-*co*-DMAM) and the fractal dimension determined therefrom. The

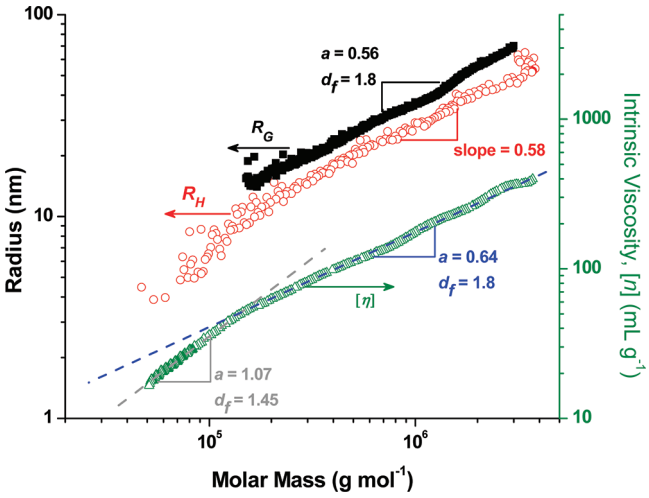

Figure 2. Chemical-heterogeneity-corrected R_G conformation plot (black filled squares), R_H conformation plot (red circles), and Mark–Houwink plot (green triangles), with slopes and fractal dimensions determined using SEC/MALS/QELS/UV/VISC/DRI. Dashed gray and blue lines denote the nonweighted first-order linear fits of the two regions of the Mark–Houwink plot, where the different slopes of the two regions indicate different fractal dimensions and, therefore, two different solution conformations, depending on M (see text for details).

calculated d_f of 1.8 (α = 0.56) corresponds to that of a linear random coil in dilute solution at thermodynamically good solvent and temperature conditions. By adding a QELS detector to our MALS/DRI combination, R_H can also be determined and plotted against molar mass to provide an R_H conformation plot. Because, as mentioned earlier, the hydrodynamic radius is a hard-sphere-equivalent radius (it may be considered the radius of a hard sphere with the same translational diffusion coefficient as the analyte),[25] a fractal dimension cannot be strictly derived from the R_H conformation plot. However, the constancy in the R_H versus M relationship observed in the plot, and the similarity between the slopes of the R_G and R_H conformation plots, together provide further support for the conclusions derived from the R_G conformation plot alone.

Using the MALS, QELS, UV, and DRI detectors online, additional architectural information about the copolymer can be gained from the measured change in the parameter ρ ($\equiv R_{G,z}/R_{H,z}$ or, more commonly, R_G/R_H, as each SEC elution slice is assumed to be virtually monodisperse) as a function of chemical-heterogeneity-corrected molar mass.[2,26] Figure 3 shows the ρ versus M relationship for the poly(AM-*co*-DMAM) copolymer. The low molar mass region, between

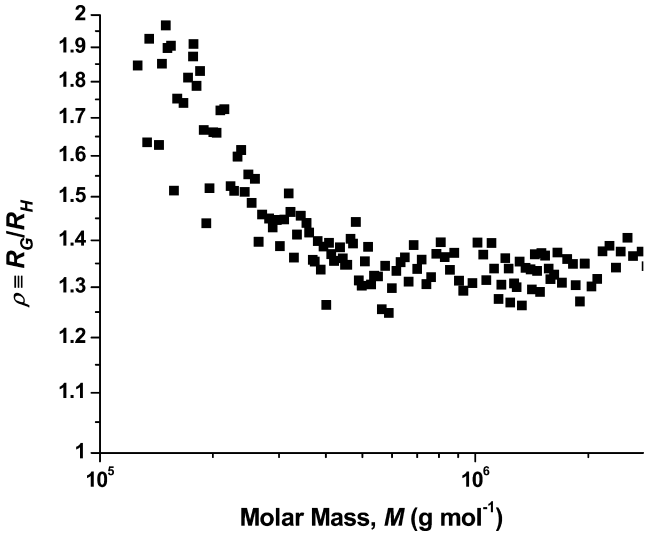

Figure 3. Plot of dimensionless size parameter ρ versus chemical-heterogeneity-corrected molar mass, determined using the MALS, QELS, UV, and DRI detectors.

1.2×10^5 g mol^{-1} and 3.7×10^5 g mol^{-1}, shows a decrease in ρ from 1.97 to 1.4 indicating that, in this region, the polymer assumes an increasingly compact conformation as a function of increasing M. At higher molar masses, i.e., in the 3.7×10^5 to 1.3×10^6 g mol^{-1} region, ρ has an essentially constant value of 1.4, indicating that the conformation attained at $M \approx 3.7 \times 10^5$ g mol^{-1} remains constant at higher M. As will be shown when discussing the Mark–Houwink and R_η/R_G plots, we believe the copolymer assumes a less flexible, more extended structure in solution at lower molar masses and transitions gradually to the more flexible, compact structure it ultimately assumes at higher M.

Figure 3 exemplifies the need for multiple detectors for properly characterizing copolymers. Were we to refer only to the R_G or R_H conformation plot, the change in conformation at lower molar masses (1.2×10^5 g mol$^{-1} \geq M \leq 3.7 \times 10^5$ g mol^{-1}) would not be noticeable. However, by combing the two radii, R_G and R_H, into ρ, we can extract a clearer picture of the conformation of this copolymer in solution and of the change in conformation as a function of M. It is clear from the ρ plot that the low molar mass end of the conformation plots encompasses a region of conformational change. It should also be mentioned that the values for ρ in Figure 3 are somewhat lower than generally expected for a linear random coil at good solvent and temperature conditions. However, while universal agreement is lacking regarding the "absolute" values of ρ, there is a general consensus about the trends in ρ with M, at a given set of solvent and temperature conditions, and about the significance of these trends with respect to changes, or lack thereof, in polymer architecture and/or conformation.[26,27]

To confirm that the copolymer becomes more compact as size increases, we use the combination of VISC, MALS, UV, and DRI to construct a chemical-heterogeneity-corrected Mark–Houwink plot of log $[\eta]$ versus log M. From this type of plot we can obtain conformational information through the well-known relation between intrinsic viscosity ($[\eta]$) and molar mass, the mutual interdependence of which is given by the Mark–Houwink equation, $[\eta] = KM^a$. As with the conformation plot, expressing this equation in logarithmic form provides the equation of a straight line:

dx.doi.org/10.1021/ac3003775 | *Anal. Chem.* 2012, 84, 4812–4820

$$\log[\eta] = a \log M + \log K \quad (6)$$

with a slope of a and a y-intercept of log K. A fractal dimension can also be calculated from the Mark–Houwink plot via the equation:[2,4]

$$d_f = \frac{3}{1 + a} \quad (7)$$

Figure 2 shows that a d_f value of 1.8 is obtained from the Mark–Houwink plot for $M > 1.25 \times 10^5$ g mol^{-1}, in excellent agreement with the d_f obtained from the R_G conformation plot. A break in the Mark–Houwink plot is observed at approximately 1.25×10^5 g mol^{-1} and, as shown in Figure 2, different power laws describe the $[\eta]$ versus M relationship above and below this point. (At this same M, a break also appears to occur in the R_H conformation plot in the same manner as it does in the Mark–Houwink plot, though R_H data below this M are too sparse and scattered to try to infer anything quantitative from them). In the 5×10^4 to 1.25×10^5 g mol^{-1} region, the d_f of the copolymer, as calculated from the Mark–Houwink plot, is 1.45, indicating a more extended structure at lower molar masses. This more extended region is not observable in the R_G conformation plot due to lack of sufficient angular dissymmetry, i.e., molecules of the copolymer with $M \leq \approx 10^5$ g mol^{-1} are not large enough to scatter light in a measurably different fashion as a function of observation angle at the given experimental conditions.[2,4,7,28] As observed earlier, however, part of the "transition region" between the two conformations adopted by the polymer is evidenced in the ρ plot given in Figure 3.

Physicochemical Basis of Architectural Changes. A trend similar to that observed in the ρ plot is also seen in the chemical-heterogeneity-corrected plot of the dimensionless parameter $R_{\eta,w}/R_{G,z}$ (or, simply, R_η/R_G, due to the aforementioned assumed virtual monodispersity of the SEC slices) versus M. The dimensionless size ratio R_η/R_G utilizes information from the combination of MALS, VISC, and DRI detectors to provide a radii ratio that is indicative of polymer conformation in solution.[2,29] Values for R_η/R_G range from approximately 0.3 to 0.4 for highly extended structures to $(5/3)^{1/2}$ for homogeneous hard spheres.[30,31] Linear random coil homopolymers generally occupy an R_η/R_G range of ≈0.7 to 0.9; the same is true of block copolymers under solvent and temperature conditions where both blocks adopt a random coil structure and is also true of random copolymers. In the latter case, however, sequence length heterogeneity can result in nonconstant values of R_η/R_G in the random coil region, due to intramolecular repulsion.[9] In the case of alternating copolymers (where, for an AB alternating copolymer, % A = % B = 50%), intramolecular repulsion is maximal and R_η/R_G values as low as ≈0.55 have been recorded.[29]

As seen in Figure 4, over the experimentally accessible R_G region, the R_η/R_G value of the copolymer increases from ≈0.55 to ≈0.75 with increasing M, at which point the value plateaus. This would appear to indicate that the more extended (although by no means rigid nor even semirigid) conformation adopted by the copolymer at lower M (confirmed by the Mark–Houwink and ρ plots in Figures 2 and 3, respectively) results from a more alternating arrangement of the AM-DAM monomers in the copolymer. The constancy in the R_η/R_G values at higher M, and the fact that the plateau region is in the expected range for random coil homopolymers, both agree with the fact, evidenced in Figure 1, that as M increases the copolymer approaches being a PDMAM homopolymer: At $M \approx 3 \times 10^5$ g mol^{-1} the % DMAM ≈ 80% and steadily approaches 100% with increasing M, while at $M > 4 \times 10^5$ g mol^{-1}, $R_\eta/R_G \approx 0.7$ for PDMAM homopolymer.

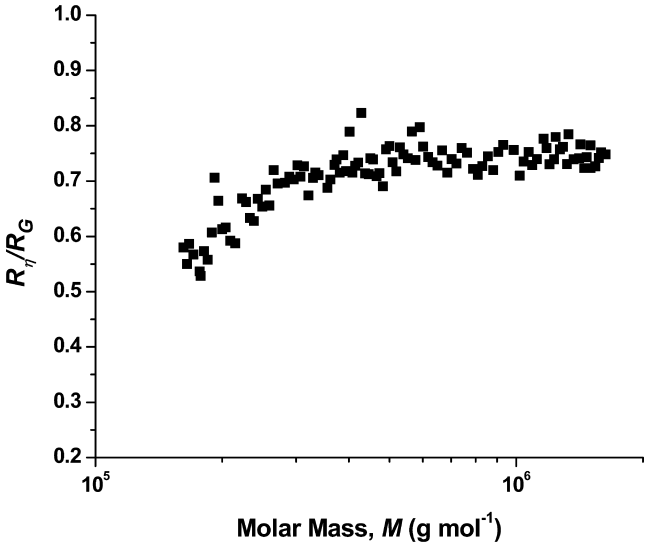

Figure 4. Plot of R_η/R_G versus molar mass, obtained using the MALS, VISC, UV, and DRI detectors. Both R_η and M have been corrected for chemical heterogeneity.

The above demonstrates the need for quintuple detection in SEC, as outlined here. MALS, VISC, and DRI detection are needed to construct Mark–Houwink and conformation plots and to determine the M-dependence of R_η/R_G; MALS and QELS are needed to determine the M-dependence of ρ; and UV, MALS, and DRI are needed to determine and correct for chemical heterogeneity.

Quantitatively, the change in conformation observed in the Mark–Houwink, ρ, and R_η/R_G plots can be understood by examining the results in terms of the persistence length (L_p) of the copolymer. This parameter corresponds to the distance a molecule extends in the direction of the initial virtual (statistical) repeat unit of the polymer backbone, averaged over all polymer conformations in solution at the given experimental conditions. Here, we determined L_p through the relation:[2]

$$\left(\frac{M}{R_G^2}\right)^{1/2} = \left(\frac{3M_L}{L_p}\right)^{1/2}\left(1 + \frac{3L_pM_L}{2M}\right) \quad (8)$$

where M_L is the molar mass per unit contour length. A plot of $(M/R_G^2)^{1/2}$ versus $1/M$ will thus have a slope of $(3/2)M_L(3L_pM_L)^{1/2}$ and a y-intercept of $(3M_L/L_p)^{1/2}$. The value of the persistence length provides an indication of chain stiffness: A large L_p is characteristic of a stiff polymer chain, while a smaller value of L_p indicates a more flexible chain. Also, in a given sample, molecules of a size greater than L_p will be more flexible than molecules of a size comparable to, or smaller than, L_p. Incorporating our experimentally obtained values of M and R_G into eq 8, the persistence length of the poly(AM-*co*-DMAM) copolymer was calculated to be 12 nm ±1 nm. On the basis of this value, and in conjunction with the previously presented architectural and conformation information about the copolymer, we hypothesize as follows: The lower-M portion of the polymer corresponds roughly to a region where $R_G \leq L_p$. In this region, the polymer assumes a more extended

dx.doi.org/10.1021/ac3003775 | *Anal. Chem.* 2012, 84, 4812–4820

(though, as mentioned earlier, not a rigid nor semirigid) conformation due to intramolecular repulsive interactions resultant from the relatively more alternating arrangement of monomers in the copolymer chain.[27] This extension is reflected in the low values of the fractal dimension d_f for this region (1.45, as compared to d_f = 1.8 in the high-M region), as obtained from the Mark–Houwink plot. We expect a transition from a less flexible to a more flexible random coil to occur at an M corresponding to an R_G of approximately 12 nm ($\approx L_p$), i.e., at $M \approx 115$ kg mol^{-1}. As seen in Figure 2, the intersection of the two power laws describing the different regions of the Mark–Houwink plot of the copolymer occurs at $M \approx 125$ kg mol^{-1}, in good agreement with expectations. The transition from less to more flexible is gradual, however, not abrupt, and this gradual transition is seen in the lower-M region of the ρ versus M and of the R_η/R_G versus M plots. The transition to a more flexible coil is expected to be complete at around $R_G \geq 2L_p$, corresponding to $M \approx 390$ kg mol^{-1}. As seen in Figures 3 and 4, ρ assumes a constant value at $M \approx 370$ kg mol^{-1} and R_η/R_G becomes constant at $M \approx 350$ kg mol^{-1}, also in good agreement with expectations. In this high-M region, the copolymer behaves more like a random coil homopolymer, as evidenced by the d_f obtained from both the conformation and Mark–Houwink plots in this region and from the plateau values of the ρ and R_η/R_G plots. The behavior in the high-M region agrees with the copolymer being 80% to 90% DMAM in this region (i.e., being close to a PDMAM homopolymer, for which ρ in this region equals 1.38 ± 0.05 and $R_\eta/R_G \approx 0.7$) and with the random coil nature of PDMAM homopolymer at the given experimental conditions.

Chemical Heterogeneity: Applications to Blends. Oftentimes, the desirable characteristics of a polymeric sample can be obtained not by copolymerizing different monomers into a copolymer but by physically combining different polymers (homo or co) in the form of a blend.[32] For instance, combining acrylonitrile-butadiene-styrene (ABS) with polyvinyl chloride (PVC) creates a blend that has good processability characteristics, derived from ABS, as well as flame resistance, derived from PVC. Blending these polymers with each other also has a synergistic effect with respect to impact strength, which is higher for the blend than it is for either of the constituent polymers.[33,34] Some advantages of blending vis-à-vis copolymerization include reduced production cost and the increased ease with which the relative ratio of the constituents can be adjusted.

In the following, we apply the quintuple-detector SEC method developed earlier to study copolymers to the characterization of 1:1 and a 1:3 blends of poly(acrylamide) and poly(*N*,*N*-dimethylacrylamide) homopolymers, the individual components of the poly(AM-*co*-DMAM) copolymer studied above. As with the copolymer, the combination of UV, DRI, and MALS was employed to calculate the ratio of the blend components as a function of molar mass, i.e., the chemical heterogeneity, shown in Figure 5 as the M-dependence of the weight percent of DMAM in the blends. Also plotted in Figure 5 is the chemical-heterogeneity-corrected differential MMD of the blends. Taken together, the MMD and chemical heterogeneity data for the 1:3 blend in Figure 5B indicate that the low and high ends of the MMD are primarily composed of PDMAM, with the sharp valley in the middle of the chemical heterogeneity plot corresponding to the location of the MMD of the PAM homopolymer. From the overlay of the chemical heterogeneity and MMD plots we can conclude

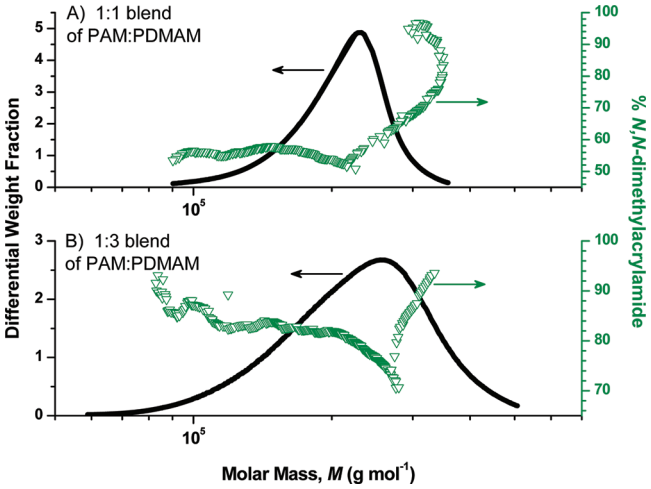

Figure 5. Molar mass distribution (corrected for chemical heterogeneity and shown as solid black lines) and chemical heterogeneity (given as percent mass fraction DMAM and shown as inverted green triangles) of two-component blends of PAM and PDMAM, determined using the MALS, DRI, and UV detectors. (A) 1:1 PAM/PDMAM, (B) 1:3 PAM/PDMAM. Upward curvature in % DMAM at high-M for the 1:1 blend and at low-M for the 1:3 blend is artifact due to low UV detector signal-to-noise ratio in this region for this blend.

that the PAM homopolymer is more narrowly disperse than is the PDMAM homopolymer, with the MMD of the former ranging from approximately 2×10^5 to 3×10^5 g mol^{-1} and that of the latter from at least 6.0×10^4 to 5.0×10^5 g mol^{-1}. These conclusions agree with the MMD of the individual homopolymer samples (not shown) and with the M_w/M_n of the homopolymers, which are 1.01 for the PAM sample and 1.25 for the PDMAM sample.

By comparison, the 1:1 blend exhibits a narrower MMD than does the 1:3 blend, as is expected due to the 1:1 blend possessing an increased amount of the narrow dispersity PAM homopolymer relative to the more disperse PDMAM. The 1:1 blend also reveals a valley in the chemical heterogeneity at $\approx 2.2 \times 10^5$ g mol^{-1}, indicating that the highest ratio of PAM to PDMAM is located at this M. However, the decrease in the % DMAM is much less pronounced for the 1:1 than for the 1:3 blend, which is also expected because of the lesser amount of PDMAM in the 1:1 blend as compared to its 1:3 counterpart.

As was the case with the copolymer, the conformation of the blend can be determined from the Mark–Houwink plot over a wider M range than can be done using the R_G conformation plot (as such, the Mark–Houwink plot is the only one shown here). As seen from the slope of the Mark–Houwink plot in Figure 6, the blend adopts the solution conformation of a linear random coil, with a d_f of 1.8 (a = 0.68). This is expected, given the known solution conformations of the individual homopolymers and that of the copolymer (Figure 2). Supporting this conclusion about the conformation of the blend is the slope of the R_η conformation plot (also shown in Figure 6), which is 0.53 and quite similar to the slopes of R_G and R_H conformation plots of the copolymer (see Figure 2). Given in Table 2 are the n-, w-, and z-statistical moments of the molar mass, viscometric and hydrodynamic radii, and intrinsic viscosity of the blend as well as the molar mass moments of the blend calculated based on the moments of the individual homopolymers and on their individual weight fractions in the blend.

dx.doi.org/10.1021/ac3003775 | Anal. Chem. 2012, 84, 4812–4820

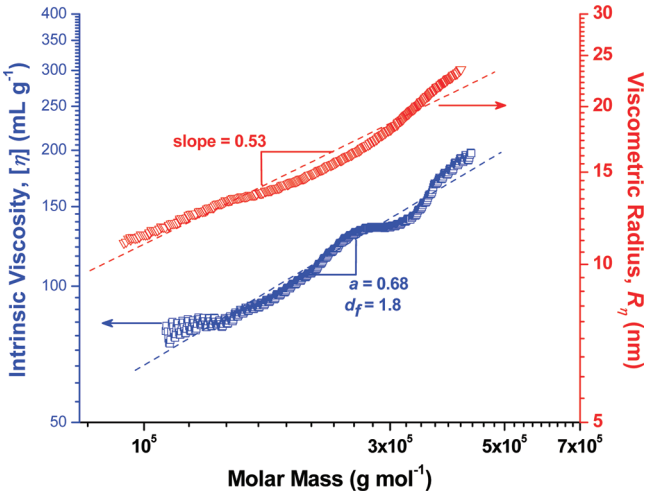

Figure 6. R_η conformation plot (red inverted triangles) and Mark–Houwink plot (blue squares) for 1:3 blend of PAM and PDMAM, as determined by SEC/MALS/VISC/UV/DRI. Both plots have been corrected for effects of chemical heterogeneity. For the Mark–Houwink plot, slope and fractal dimension correspond to those of an unweighted first-order linear fit (shown as dashed blue line) with r = 0.985. Fluctuations in the plots reflect partial overlap of the MMDs of the component homopolymers.

CONCLUSIONS

A five-detector SEC method was introduced to characterize copolymers and blends the components of which have overlapping UV absorption spectra. Application of this multidetector technique to the study of a copolymer of acrylamide and *N*,*N*-dimethylacrylamide, and to blends of the constituent homopolymers, allowed for quantitation of the chemical heterogeneity, of the chemical-heterogeneity-corrected molar mass averages and distribution, intrinsic viscosity, and macromolecular radii, and of the solution conformation of the analytes. The need for the five detectors was evidenced throughout, most notably when studying the *M*-dependence of the copolymer conformation and the physicochemical basis thereof: The poly(AM-*co*-DMAM) was seen to adopt a less flexible random coil structure at lower *M*, proceeding through a transition region into a more flexible random coil structure which remained constant at higher *M*. Physically, this change in conformation was attributed to the relative size of the polymer in each regime, as compared to the persistence length L_p of the copolymer at the given experimental conditions. Chemically, the relative extension or flexibility of the macromolecule appears to be due to a combination of chemical heterogeneity, which accounts for the near-homopolymeric structure and related random coil nature of the higher-*M* chains and of intrachain monomeric arrangement, which results in a more alternating-like structure of the copolymer at lower-*M*, with concomitantly higher intrachain repulsion and, hence, a higher degree of chain extension as compared to the higher-*M* chains. The quintuple-detector approach allowed for *all* of the above to be determined in a single analysis, with similar characterization being effected for 1:1 and 1:3 blends of PAM and PDMAM.

The experimental method and equations presented here are not specific to the copolymer and blends studied. Rather, they can be applied to any copolymer or binary blend in which either one or both of the constituents absorb in the UV region of the electromagnetic spectrum. Similarly, size-based separation techniques other than SEC, such as hydrodynamic chromatography or field-flow fractionation,[35−37] can be used as well, though accurate coupling of a viscometer to a field-flow fractionation channel is not possible with current technology. Given the large number of materials properties affected by chemical heterogeneity, molar mass, polymeric architecture, etc., and because the experiments rely on separation and detection methods common to most macromolecular separations laboratories, the method presented should benefit those interested in the design, synthesis, processing, and/or end-uses of macromolecules, both natural and synthetic.

ASSOCIATED CONTENT

Supporting Information

Additional information as noted in text. This material is available free of charge via the Internet at http://pubs.acs.org.

AUTHOR INFORMATION

Corresponding Author

*E-mail: andre.striegel@nist.gov.

Notes

The authors declare no competing financial interest.

ACKNOWLEDGMENTS

The authors would like to thank Drs. Imad Haidar Ahmad and Kevin N. Sill for helpful advice during the initial stages of this project. The identification of certain commercial equipment, instruments, or materials does not imply recommendation or endorsement by the National Institute of Standards and Technology. These identifications are made only in order to specify the experimental procedures in adequate detail.

REFERENCES

(1) Moore, J. C. *J. Polym. Sci., Part A* **1964**, *2*, 835−843.

Table 2. Molar Mass, R_η, R_H, and $[\eta]$ Statistical Moments of a 1:3 Blend of PAM and PDMAM, As Determined by SEC/MALS/QELS/VISC/UV/DRI

	number-average	weight-average	*z*-average
M_{exp} (g mol^{-1})[a]	$2.10 \times 10^5 \pm 0.10 \times 10^5$	$2.37 \times 10^5 \pm 0.08 \times 10^5$	$2.64 \times 10^5 \pm 0.05 \times 10^5$
M_{calc} (g mol^{-1})[b]	$1.96 \times 10^5 \pm 0.09 \times 10^5$	$2.36 \times 10^5 \pm 0.09 \times 10^5$	$2.76 \times 10^5 \pm 0.16 \times 10^5$
R_H (nm)[c]	12 ± 1	13 ± 1	14 ± 2
R_η (nm)[c]	15 ± 1	16 ± 1	17 ± 1
$[\eta]$ (mL g^{-1})[c]	109 ± 5	119 ± 3	129 ± 2

[a]Experimentally determined *M* averages for blend. [b]Molar mass averages calculated based on *M* averages of individual homopolymers and weight fraction of each homopolymer in the blend. [c]Experimentally determined values, at solvent and temperature conditions as specified in the Experimental Section. Standard deviations based on replicate injections from duplicate dissolutions, as specified in the Experimental Section.

dx.doi.org/10.1021/ac3003775 | *Anal. Chem.* 2012, 84, 4812−4820

(2) Striegel, A. M.; Yau, W. W.; Kirkland, J. J.; Bly, D. D. *Modern Size-Exclusion Liquid Chromatography: Practice of Gel Permeation and Gel Filtration Chromatography*, 2nd ed.; Wiley: Hoboken, NJ, 2009.
(3) Striegel, A. M., Ed. *Multiple Detection in Size-Exclusion Chromatography*; ACS Symposium Series 893; American Chemical Society: Washington, DC, 2005.
(4) Striegel, A. M. *Anal. Chem.* **2005**, *77*, 104A−113A.
(5) Striegel, A. M. *Anal. Bioanal. Chem.* **2008**, *390*, 3003−3005.
(6) Ouano, A. C.; Kaye, W. *J. Polym. Sci. Polym. Chem. Ed.* **1974**, *12*, 1151−1162.
(7) Wyatt, P. J. *Anal. Chim. Acta* **1993**, *272*, 1−40.
(8) Benkoski, J. J.; Fredrickson, G. H.; Kramer, E. J. *J. Polym. Sci., Part B: Polym. Phys.* **2001**, *39*, 2363−2377.
(9) Stejskal, J. *Polym. Int.* **2005**, *54*, 108−113.
(10) Viridén, A; Wittgren, B.; Andersson, T.; Larsson, A. *Eur. J. Pharm. Sci.* **2009**, *36*, 392−400.
(11) Yeung, C.; Balazs, A. C.; Jasnow, D. *Macromolecules* **1992**, *25*, 1357−1360.
(12) Haidar Ahmad, I. A.; Striegel, A. M. *Anal. Bioanal. Chem.* **2010**, *399*, 1589−1598.
(13) Netopilík, M.; Behdanecký, M; Kratochvíl, P. *Macromolecules* **1996**, *29*, 6023−6030.
(14) Kang, S.; Vogt, B. D.; Wu, W.; Prabhu, V. M.; VanderHart, D. L.; Rao, A.; Lin, E. K.; Turnquest, K. *Macromolecules* **2007**, *40*, 1497−1503.
(15) Hiller, W.; Sinha, P.; Hehn, M.; Pasch, H.; Hofe, T. *Macromolecules* **2011**, *44*, 1311−1318.
(16) Lodefier, P.; Jonas, A. M.; Legras, R. *Macromolecules* **1999**, *32*, 7135−7139.
(17) Montaudo, M. S. In *Multiple Detection in Size-Exclusion Chromatography*; Striegel, A. M., Ed.; ACS Symposium Series 893; American Chemical Society: Washington, DC, 2005; pp 152−167.
(18) Braun, D.; Krämer, I.; Pasch, H.; Mori, S. *Macromol. Chem. Phys.* **1999**, *200*, 949−954.
(19) Medrano, R.; Laguna, M. T. R.; Saiz, E.; Tarazona, M. P. *Phys. Chem. Chem. Phys.* **2003**, *5*, 151−157.
(20) Trainoff S. Method for correcting the effects of interdetector band broadening. U.S. Patent 7,386,427, June 10, 2008.
(21) Brusseau, R. J.; Goetz, N.; Machtle, W.; Stoelting, J. *Tenside, Surfactants, Deterg.* **1984**, *28*, 396−406.
(22) Berkowitz, S. A. *J. Liq. Chromatogr.* **1983**, *6/8*, 1359−1373.
(23) Michielsen, S. In *Polymer Handbook*, 4th ed.; Brandup, J., Immergut, E. H., Eds.; Wiley: New York, 1999; pp VII/547−VII/627.
(24) Haidar Ahmad, I. A.; Striegel, A. M. *Instrum. Sci. Technol.* **2009**, *37*, 574−583.
(25) Smith, M. J.; Haidar, I. A.; Striegel, A. M. *Analyst* **2007**, *132*, 455−460.
(26) Burchard, W *Adv. Polym. Sci.* **1999**, *143*, 113−194.
(27) Konishi, T.; Yoshizaki, T.; Yamakawa, H. *Macromolecules* **1991**, *24*, 5614−5622.
(28) Brewer, A. K.; Striegel, A. M. *Anal. Bioanal. Chem.* **2011**, *399*, 1507−1514.
(29) Haidar Ahmad, I. A.; Striegel, D. A.; Striegel, A. M. *Polymer* **2011**, *52*, 1268−1277.
(30) Ostlund, S. G.; Striegel, A. M. *Polym. Degrad. Stab.* **2008**, *93*, 1510−1514.
(31) Striegel, A. M. *Biomacromolecules* **2007**, *8*, 3944−3949.
(32) Paul, D. R., Newman, S., Eds. *Polymer Blends*, Vol. *1*; Academic Press: New York, 1978.
(33) Weber, M. *Macromol. Symp.* **2001**, *163*, 235−250.
(34) Yen, C. S.; Hassan, A.; Hashim, S. *J. Teknol.* **2003**, *39*, 107−116.
(35) Striegel, A. M.; Brewer, A. K. *Annu. Rev. Anal. Chem.* **2012**, *5*, 15−34.
(36) Striegel, A. M. *Anal. Bioanal. Chem.* **2012**, *402*, 77−81.
(37) Podzimek, S. *Light Scattering, Size Exclusion Chromatography and Asymmetric Flow Field Flow Fractionation*; Wiley: Hoboken, NJ, 2011.

The Characterization of Copolymers and Blends by Quintuple-Detector Size-Exclusion Chromatography

Steven M. Rowland[a] **and André M. Striegel**[*,b]

[a]*Department of Chemistry & Biochemistry, Florida State University, Tallahassee, FL 32306-4390,* [b]*Analytical Chemistry Division, National Institute of Standards and Technology, 100 Bureau Drive, Mail Stop 8392, Gaithersburg, MD 20899*

Given herein is a detailed derivation of equation 2 of the manuscript, employed to quantitate the chemical heterogeneity in a dual-absorbing copolymer or binary blend. Also included is a representative QELS correlation function for the copolymer, obtained with the QELS detector coupled to the SEC system as described in the Experimental.

[*] Corresponding author. E-mail: andre.striegel@nist.gov

Supplementary Information. Derivation of equation 2 for chemical heterogeneity in a dual-absorbing copolymer or binary blend.

To relate the results given here to the copolymers and blends studied in the manuscript, the derivation of equation 2 will be given in terms of the poly(AM-*co*-DMAM) copolymer (referred in this **Supplementary Information** only as "*Copolymer*") studied but are, of course, universal to any copolymer in which both functionalities have overlapping absorbances in the UV region or to any binary blend in which the UV absorbances of both components overlap. The results apply not only to SEC but also to any type of size-based separation, such as hydrodynamic chromatography or certain field-flow fractionation methods.

Determination of chemical heterogeneity (which will ultimately be given in terms of the percent mass fraction *N,N*-dimethylacrylamide, %DMAM, as in equation 2), relies on the use of two concentration-sensitive detectors, a DRI and a UV. The concentration-sensitivity of each of these detectors is given by:

$$S_{DRI,i} = k_{DRI} \times C_{Copolymer,i} \times \left[\left(\frac{\partial n}{\partial c} \right)_{PAM} w_{AM,i} + \left(\frac{\partial n}{\partial c} \right)_{PDMAM} w_{DMAM,i} \right] \quad \text{(S1)}$$

$$S_{UV,i} = k_{UV} \times b \times \left(a_{PAM} \times C_{AM,i} + a_{PDMAM} \times C_{DMAM,i} \right) \quad \text{(S2)}$$

where, for each SEC elution slice i, C is concentration; S_{DRI} is the signal from the DRI; k_{DRI} is the instrument constant for the DRI detector; $(\partial n/\partial c)_{PAM}$ and $(\partial n/\partial c)_{PDMAM}$ are the specific refractive index increments of the PAM and PDMAM homopolymers, respectively; and $w_{AM,i}$ and $w_{DMAM,i}$ are, respectively, the weight fractions of the acrylamide and *N,N*-dimethylacrylamide components of the copolymer. Using equation 1, equation S1 can be rewritten as $S_{DRI,i} = k_{DRI} \times C_{Copolymer,i} \times (\partial n/\partial c)_{Copolymer,i}$. The signal from the UV detector at each elution slice, $S_{UV,i}$, is given by Beer's law, in which k_{UV} is the instrument constant; b is the UV cell path length; a_{PAM} and a_{PDMAM} are the absorptivities of the polyacrylamide and poly(*N,N*-dimethylacrylamide)

homopolymers, respectively; and $C_{AM,i}$ and $C_{DMAM,i}$ are, respectively, the concentrations of acrylamide and *N,N*-dimethyl acrylamide in the slice. Note that comparison of slice-wise data among different detectors follows correction for interdetector delay and interdetector band broadening, as outlined in the **Experimental** section.

Because the chemical composition at each slice, i.e., the relative monomer (or blend component) ratio at each elution slice, is obtained from the ratio of S_{UV} to S_{DRI}, we give this ratio the symbol $S_{R,i}$ and define it as:

$$S_{R,i} = \frac{S_{UV,i}}{S_{DRI,i}} \tag{S3}$$

If we also term the ratio of the UV and DRI instrument constants (k_{UV} and k_{DRI}, respectively) k_R and define it as:

$$k_R = \frac{k_{UV}}{k_{DRI}}$$

then

$$S_{R,i} = k_R \times \frac{b \times k_{UV,off} \times \left(a_{PAM} \times C_{AM,i} + a_{PDMAM} \times C_{DMAM,i}\right)}{C_{Copolymer,i} \times \left(\frac{\partial n}{\partial c}\right)_{Copolymer,i}} \tag{S4}$$

where $k_{UV,off}$ is the instrument constant for the off-line UV spectrophotometer employed to determine the absorptivities of the homopolymers. The instrument constant ratio k_R can be determined by analyzing a homopolymeric sample of one of the components of the copolymer or blend. We chose to analyze the homopolymer PDMAM, so that:

$$k_R = S_{R,PDMAM} \times \frac{\left(\frac{\partial n}{\partial c}\right)_{PDMAM}}{b \times k_{UV,off} \times a_{PDMAM}} \tag{S5}$$

Because %DMAM is always 100% for a sample of PDMAM homopolymer, $S_{R,i}$ will be constant for this sample, i.e., for a homopolymer $S_{R,i} = S_R$. This same is true for the specific refractive index increment and for the absorptivity of a homopolymer (assuming negligible oligomeric

content), thus allowing us to combine the PDMAM-specific constants in equation S5 into the term Z_{PDMAM}:

$$Z_{PDMAM} = S_{R,PDMAM} \times \frac{\left(\frac{\partial n}{\partial c}\right)_{PDMAM}}{a_{PDMAM}} \tag{S6}$$

Now, the instrument constant ratio k_R can be rewritten as:

$$k_R = \frac{Z_{PDMAM}}{b \times k_{UV,off}} \tag{S7}$$

By then substituting for k_R, we eliminate the need to determine the instrument constants for the UV and DRI detectors and also cancel the UV cell path length b and the instrument constant for the off-line UV spectrophotometer $k_{UV,off}$ out of equation S4, which now takes the form:

$$S_{R,Copolymer,i} = Z_{PDMAM} \times \frac{C_{DMAM,i} \times a_{PDMAM} + C_{AM,i} \times a_{PAM}}{C_{Copolymer,i} \times \left(\frac{\partial n}{\partial c}\right)_{Copolymer,i}} \tag{S8}$$

The individual ratios of C_{DMAM} and C_{AM} to $C_{Copolymer}$ each provide the respective weight fraction w of DMAM and AM at each slice i:

$$w_{DMAM,i} = \frac{C_{DMAM,i}}{C_{Copolymer,i}} \tag{S9a}$$

and

$$w_{AM,i} = \frac{C_{AM,i}}{C_{Copolymer,i}} \tag{S9b}$$

Incorporating equations 1 and S9 into equation S8 allows the latter to be rewritten as:

$$S_{R,Copolymer,i} = Z_{PDMAM} \times \frac{w_{DMAM,i} \times a_{PDMAM} + w_{AM,i} \times a_{PAM}}{w_{DMAM,i} \times \left(\frac{\partial n}{\partial c}\right)_{PDMAM} + w_{AM,i} \times \left(\frac{\partial n}{\partial c}\right)_{PAM}} \tag{S10}$$

Because there are only two monomer types in the type of copolymer studied (or two components in a binary blend), the sum of their weight fractions must equal unity, i.e., $w_{DMAM} + w_{AM} = 1$, and w_{AM} can be rewritten as $1 - w_{DMAM}$, so that:

$$S_{R,Copolymer,i} = Z_{PDMAM} \times \frac{w_{DMAM,i} \times a_{PDMAM} + \left(1 - w_{DMAM,i}\right) \times a_{PAM}}{w_{DMAM,i} \times \left(\frac{\partial n}{\partial c}\right)_{PDMAM} + \left(1 - w_{DMAM,i}\right) \times \left(\frac{\partial n}{\partial c}\right)_{PAM}} \quad \text{(S11)}$$

Solving equation S11 for $w_{DMAM,i}$ and multiplying both sides by 100% provides equation 2, the percent mass fraction of DMAM at each elution slice i (%DMAM$_i$) in the SEC-separated copolymer (or blend). The percent mass fraction of the acrylamide (%AM) component can be calculated at each elution slice from the relation %AM$_i$ = 100% - %DMAM$_i$.

Representative QELS autocorrelation function of P(AM-*co*-DMAM), obtained by SEC/QELS